

**S. Table 1** Crystal information and Ni-P-H MOF structure refinement parameters.

Empirical formula	Formula weight	Crystal system	Space group	<i>a</i> (Å)	<i>b</i> (Å)	<i>c</i> (Å)	<i>V</i> (Å <sup>3</sup> )	<i>Z</i>	<i>D<sub>c</sub></i> (g cm <sup>-3</sup> )	<i>μ</i> (mm <sup>-1</sup> )
C <sub>7</sub> H <sub>17</sub> NNiO <sub>11</sub>	349.92	Orthorhombic	Pna2 <sub>1</sub>	15.747 3 (8)	11.706 0 (6)	7.0023 (3)	1290.80 (11)	4	1.802	1.56
<b>θ range (°)</b>	<b>Measured refls.</b>	<b>Independent refls.</b>	<b><i>R</i><sub>int</sub></b>	<b><i>S</i></b>	<b><i>R</i><sub>1</sub>/<i>wR</i><sub>2</sub></b>	<b>Δρ<sub>max</sub>/Δρ<sub>min</sub> (eÅ<sup>-3</sup>)</b>				
2.6-26.5	15823	2662	0.045	1.04	0.029/0.063	0.30/-0.42				

**S. Table 2** Selected bond distances and angles for complexes **1** (Å, °)

**Table 2** Selected bond distances and angles (Å, °)

N1—Ni1	2.106(2)	Ni1—O5	2.016(3)
Ni1—O8	2.106(3)	Ni1—O9	2.072(2)
O5—Ni1—O7	174.13(16)	O5—Ni1—O6	91.73(12)
O6—Ni1—N1	88.42(13)	O9—Ni1—N1	176.5(2)

**S. Table 3.** Hydrogen-bond parameters for complex **1** (Å, °)

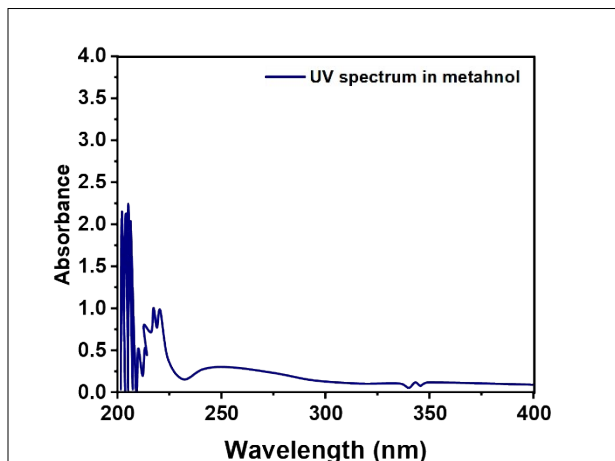
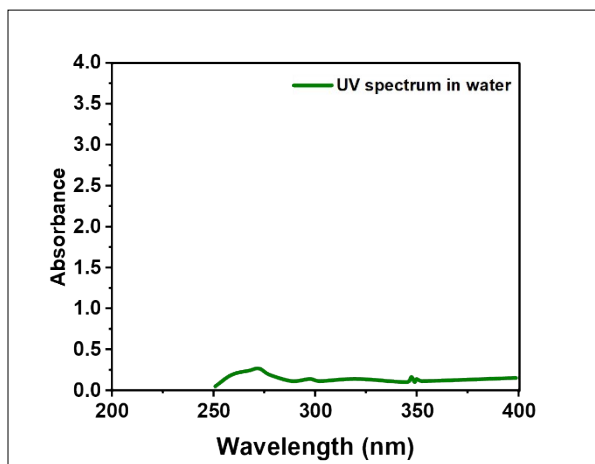
D—H···A	D—H	H···A	D···A	D—H···A
O5—H5A···O3 <sup>(x-1/2, -y+1/2, z)</sup>	0.84 (2)	1.89 (2)	2.698 (4)	159
O5—H5B···O11 <sup>(-x+1, -y+1, z+1/2)</sup>	0.80 (2)	1.98 (2)	2.734 (4)	155
O6—H6A···O1 <sup>(-x+1/2, -y+1, z)</sup>	0.83 (2)	1.91 (2)	2.727 (4)	168

$y-1/2, z-1/2;$				
O6—H6B···O11 <sup>(-x+1,</sup> $-y+1, z-1/2;)$	0.80 (2)	1.92 (2)	2.722 (4)	173
O7—H7A···O10 <sup>(-x+1,</sup> $-y+1, z-1/2;)$	0.80 (2)	1.99 (3)	2.767 (5)	164
O7—H7B···O4 <sup>(-x+1/2,</sup> $y+1/2, z-1/2;)$	0.80 (2)	1.94 (3)	2.718 (4)	163
O8—H8A···O2 <sup>(x-1/2,</sup> $-y+3/2, z;)$	0.84 (2)	1.82 (2)	2.656 (4)	178
O8—H8B···O4 <sup>(-x+1/2,</sup> $y+1/2, z+1/2)$	0.83 (2)	2.16 (3)	2.905 (4)	149
O9—H9A···O1 <sup>(x-1/2,</sup> $-y+3/2, z;)$	0.79 (2)	2.02 (2)	2.807 (3)	169
O9—H9B···O4 <sup>(x-1/2,</sup> $-y+1/2, z;)$	0.80 (2)	2.05 (2)	2.854 (3)	173
O10—H10A···O3	0.83 (2)	1.84 (2)	2.659 (4)	173
O10—H10B···O6 <sup>(x+1/2,</sup> $-y+1/2, z)$	0.82 (2)	2.50 (3)	3.076 (4)	128
O10—H10B···O8 <sup>(-x+1,</sup> $-y+1, z-1/2;)$	0.82 (2)	2.37 (3)	2.983 (4)	132
O11—H11A···O10	0.83 (2)	1.87 (2)	2.701 (3)	178
O11—H11B···O2	0.80 (2)	1.93 (3)	2.684 (3)	157

## 1.0. UV visible analysis of Ni-P-H MOF

The ligand 1,2,4,5 BTA had a peak absorbance of 4.00 at 229.2 nm when analyzed in water. To study the UV-visible properties of the Ni-P-H MOF (complex), 1 mg of the MOF was dissolved in 5 ml of water and methanol to yield a clear solution. Following that, the solutions were sonicated for 5 minutes. The peak absorbance of the complex in water was at 269 nm with a value of 0.232, and in methanol, it was at 252.5 nm with a value of 0.292. This suggests that the transitions in the complex are in the ultraviolet region, likely due to  $n \rightarrow \pi^*$  transitions, which typically have low

energy and longer wavelengths. The peak absorbance in both solvents was larger than that of the ligand, suggesting that the complex displayed a red shift or bathochromic shift, most likely as a result of metal-ligand interaction. This longer wavelength shift confirms the formation of the complex. The complex's UV-visible spectrum in both water and methanol is depicted in the figure.



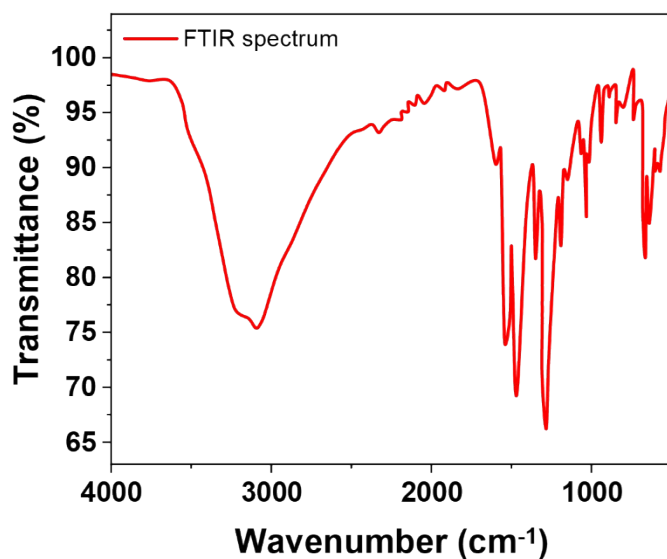
S. Figure 1. UV Spectra of Ni-P-H MOF in a) water

b) methanol

## 2.0 FTIR spectrum of Ni-P-H MOF

The Ni-P-H MOF spectra displayed a number of novel peaks and functional group band changes to lower wavenumber. The first broad peak at  $3127\text{ cm}^{-1}$  was identified as the peak of water molecule due to the O-H stretching. However, this peak shifted from a lower frequency of  $394\text{ cm}^{-1}$ , indicating that water molecules were entrapped within the complex. Furthermore, it was discovered that the C=O bond's stretching vibrations were in the  $1555\text{-}1435\text{ cm}^{-1}$  range, with a 53-

74  $\text{cm}^{-1}$  blue shift, indicating the metal-ligand coordination. Another hump due to the presence of C-O group in the structure of carboxylic acid was detected in the 1369-1125  $\text{cm}^{-1}$  range, and moved to 41-119  $\text{cm}^{-1}$  which is the lower frequency region, further indicating metal-carboxylic coordination. These spectral shifts show a significant divergence between the complex and ligand spectra, proving complex formation has taken place.



S. Fig. 2.

The table below includes a list of all of the components' major frequencies

Ni-P-H MOF (cm <sup>-1</sup> )	Ligand (cm <sup>-1</sup> )	Assignment
3127	3521-3055	(O-H)
1555	1666	(C=O)
1435-1369	1509-1411	(C-O)
1125	1114	(C-C)
763	-	(M-N)

560	-	(M-O)
-----	---	-------

### 3.0. Fluorescence Analysis

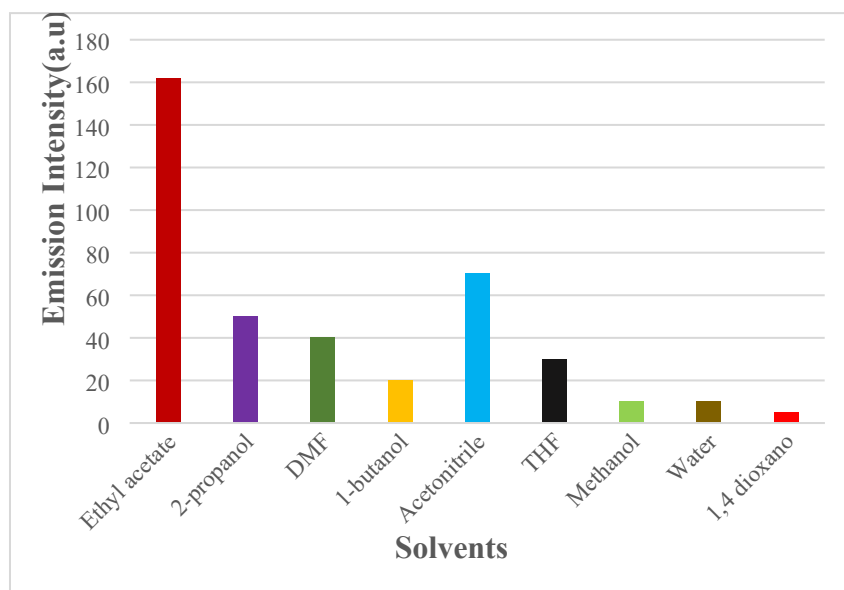
Fluorescence can be described in terms of the absorbance of light by atoms or molecules followed by their re-emission by them with a shift towards higher wavelength. Transition metal complexes, which have partially filled d-orbitals, are responsible for controlling the behavior of these atoms or molecules. The properties of absorption and emission are determined by the occupation and organization levels of these orbitals, and the spectroscopic state of the atoms or molecules is also influenced by their orbital configuration. In fluorescence experiments, researchers commonly examine three primary excited states: the  $\pi$  to  $\pi^*$  ligand base state, charge transfer state, and d-d state. The excitation of the first state is generated by the transfer one d-electron to the other d-electronic state. The transition of an electron to the  $\pi$ -orbital to a metal d-orbital which is empty leads to the recording of the second excited state or the promotion of a d-electron to the  $\pi^*$  orbital. The third excited state is entered when an electron is transferred from a bonding to a non-bonding orbital.

#### 3.1. Solvent effect

The choice of solvent used in a procedure can greatly affect the fluorescence activity of a substance. Polar solvents, which have a dipole moment, interact with fluorophores, leading to the gain of energy and transition to a higher energy level, and also resulting in the relaxation of solvent molecule. This causes fluorophore's dipole moment to change and the solvent molecules to rearrange, which enables the emission spectrum to experience a red shift. The difference between the excited and ground states of coordination compounds is widened by non-polar solvents, which causes shorter wavelength emissions and a blue shift in the observed emission bands. The use of different solvents can also cause changes in intensity in the final spectra, leading to either an increase or decrease in emission intensity.

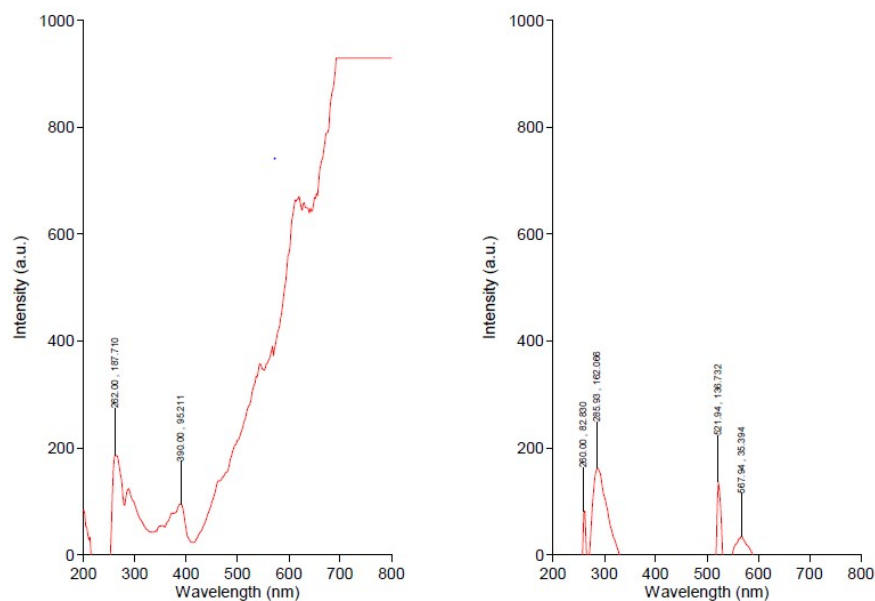
### 3.2. Solvent selection for Ni-P-H MOF

A sample suspension was created by sonication in various solvents, including dimethyl formamide, methanol, and ethyl acetate. The Agilent Technologies Cary Eclipse Fluorescence spectrophotometer was used to measure the intensity of the suspensions at various wavelengths. After comparing the results, ethyl acetate was determined to be the optimal solvent as it had the highest intensity. This solvent was then used for further studies.



The Ni-P-H MOF displayed the strongest intensity when dissolved in ethyl acetate. Upon being excited by a 260nm wavelength, it emitted a 285nm wavelength with an intensity of 162 (a.u). The

complex 2 also emitted a red light, which was caused by a weak transition from the electron transfer from the aromatic ring of the ligand to the metal.

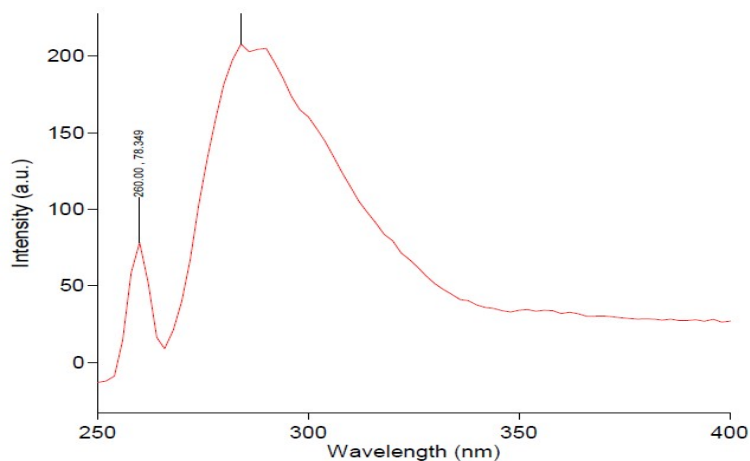


#### 4.0 Fluorescent PH sensing properties of complexes

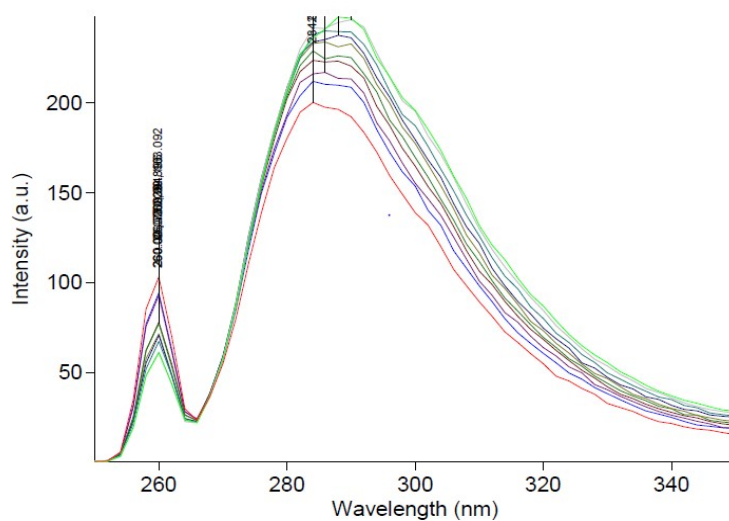
Fluorescent pH sensors have many advantages over traditional electrodes and can be used in various fields such as environmental analysis, bioanalytical chemistry, and medicine. Researchers have studied the pH-dependent fluorescence of complexes due to their stability over a wide range of pH levels. Different acidic environments were utilized to measure the fluorescence emission intensity of these complexes.

##### 4.1 Fluorescent PH sensing property of Ni-P-H MOF

The fluorescence stability of a complex was examined before conducting spectroscopy at different pH levels. The fluorescence spectrum was monitored as the pH of a solution was altered, and a second measurement was taken 10 minutes later to confirm stability. The results indicate that the complex remains stable as the emission intensity at 200 nm ( $I_{Eu}$ ) remains consistent across all pH solutions.

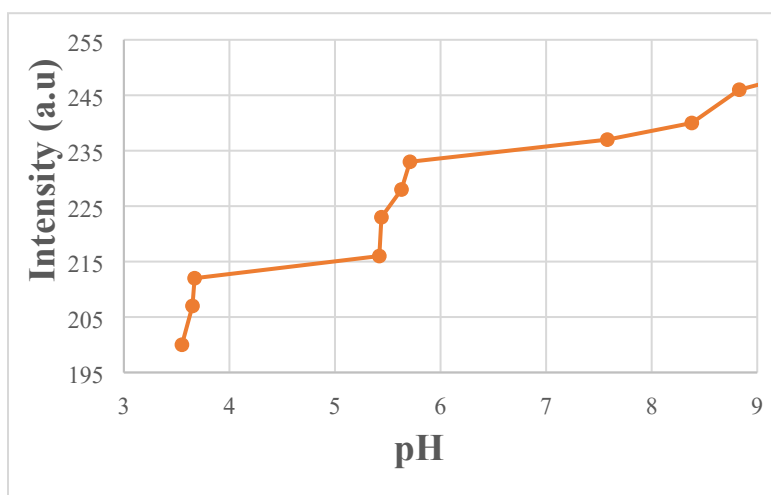


The pH sensing properties of complex 1, known as Ni-P-H-MOF, were studied by measuring its fluorescence spectra in various pH solutions. The intensity of the emission peaks altered as the sample's pH fluctuated, but their position, range, and shape remained consistent. The fluorescence was brightest in the most basic solution and weakest in the most acidic solution. The amount of coordination sites on the ligand in various pH conditions and the energy transfer and return effect between the metal and ligand both have an impact on the change in emission intensity. COOH-groups, that are capable to exist in the deprotonated state (COO<sup>-</sup>) possess higher activity in solution towards metal ions, are present on the surface of the complex. As the pH rises, it can be seen that the number COO<sup>-</sup> groups and coordination sites increases on the surface of the ligand, which leads to a greater number of Ni-ions coordinating to a stronger emission as well as 1,2,4,5 BTA. The Ni and 1,2,4,5 BTA energy transfer and return effect also contributes to the fluorescence intensity.

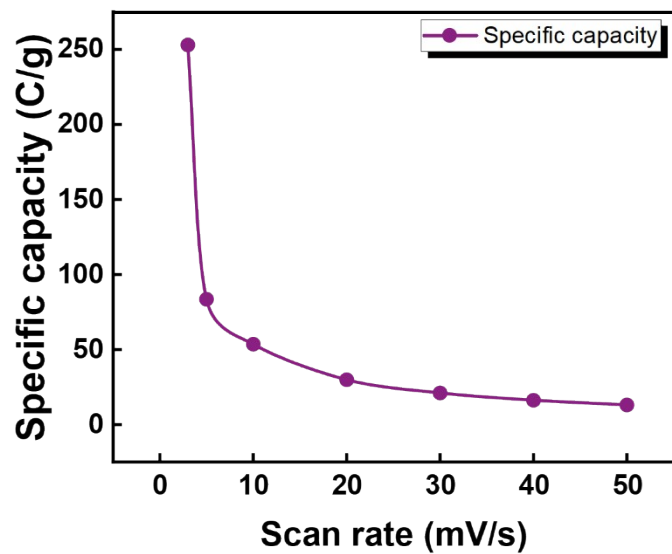




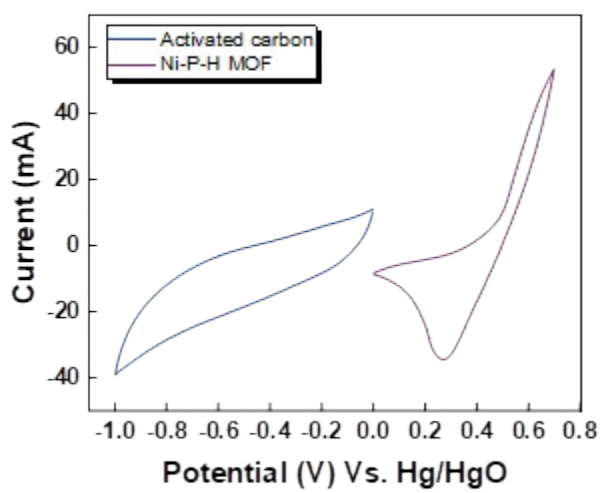
<b>PH value</b>	<b>Intensity (a.u)</b>
3.55	200
3.65	207
3.67	212
5.42	216
5.45	223
5.63	228
5.71	233
7.58	237
8.38	240
8.83	246
9.03	247



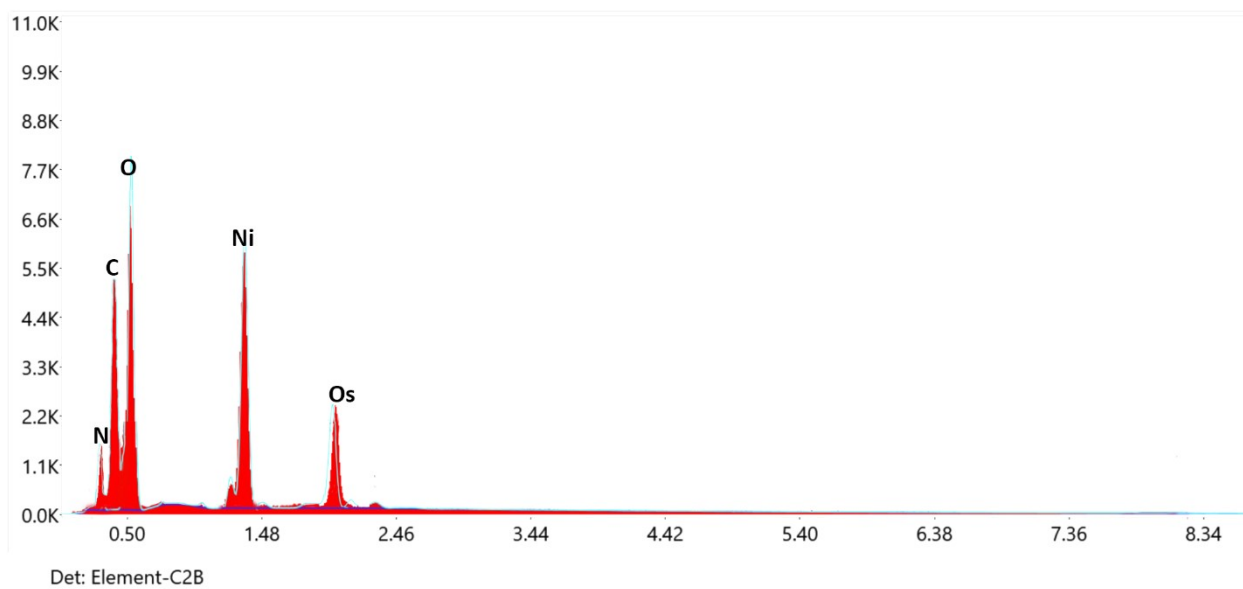
$I_{EU}$  vs. pH curve of Ni-P-H MOF



S. Fig. 3.



S. Fig. 4



**S.Fig. 5. EDX of Ni-P-H MOF**